Novel Parameter Estimation Method for Chirp Signals Using Bowtie Chirplet and Discrete Fractional Fourier Transform

Ahmed Mostayed[1], Saurav Zaman Khan Sajib[2] and Sikyung Kim[3]
[1,2]*Department of Electrical Engineering, Kongju National University, Kongju, Korea*
E-mail: shaibal125@yahoo.com[†], *sajib127@hotmail.com*[††], *skim@kongju.ac.kr*[3]

Abstract

A new parameter estimation method for linear chirp signal is proposed. This method utilizes the Discrete Fractional Fourier Transform (DFRFT) along with Bowtie Chirplet Transform to estimate the amplitude and phase parameters of multi-component chirp signals. DFRFT is used for estimating amplitude parameter whereas the chirp rate and initial frequency are estimated using Chirplet Transform. Performance of the proposed method in noise is analyzed by Monte-Carlo simulation for different Signal to Noise Ratio (SNR). Good performance was achieved at SNR as low as -10 dB.

1. Introduction

Polynomial Phase Signals (PPS), especially linear chirp signals are frequently used in Mobile communications, Sonar and Synthetic Aperture Radar (SAR) imaging of moving targets and geophysics. It is well known that the radar echo of a moving target with constant acceleration is a chirp signal. By estimating the chirp rate and initial frequency of the received signal, one can achieve valuable information about the velocity and acceleration of the target. In such applications the amplitude of the chirp signal is considered as a nuisance parameter which does not contain any significant information. A more recent application of linear chirp signals have been investigated for speech signals with multi-component linear amplitude modulated chirp signals [1]. In that case, the amplitude parameters are as important as the chirp rates and initial frequencies of component signals. Hence, techniques that estimate the phase parameters (Initial frequency and chirp rate) as well as amplitude parameters accurately under noisy environment are needed to be established.

In the early nineties the time-frequency analysis based on Wigner–Ville (WVD) distribution was applied for detection and imaging of moving objects with SAR [2]. But the cross-term associated with Wigner distribution hampers the estimation performance in extreme noisy conditions. However, the time-frequency analysis is restricted to applications where chirp rate is the only parameter of interest. To overcome that, the Radon Transform of WVD (RTW or RWT) was proposed by Wood [3]. This method is based on the line integral of the time-frequency plane along all possible lines and the outcome of the transform is localized maxima on the initial phase-chirp rate plane. The computational complexity of RTW was reduced by Wang [4] employing the Radon transform of the ambiguity function (2D FFT of WVD), well known as RAT. RAT limits the line integral to lines passing through the origin hence losing information about the initial frequency parameter. A sequential estimation procedure is proposed by Zhao [5] which employs RAT to estimate chirp rate and Fractional Fourier transform (FRFT) [6, 7] to estimate amplitude and initial frequency. But this method is restricted to constant amplitude chirps only. In fact conventional FRFT based method is useful for mono-component constant amplitude chirp signals. But presence of

multi-component signals and high amplitude difference between them make it extremely difficult to estimate parameters accurately. Moreover, with those methods the signal has to be investigated over the full range of [0, 2π]. Methods based on wavelet [8, 9] and Discrete Polynomial Phase Transform (DPT) are also reported [10]. Some recent works involve Discrete chirp Fourier transform for chirp rate estimation [11], and slope calculation of ambiguity function for parameter estimation [1] etc.

In this paper a new sequential estimation method for linear chirp signals are proposed. The method is based on Bowtie Chirplet and Discrete Fractional Fourier transforms (DFRFT). The Ability of Bowtie Chirplet transform to localize even in high noise condition ensures highly accurate estimation of chirp rate and initial frequency. Furthermore the inherent chirp compaction property of DFRFT for optimal domain can be effectively used to estimate amplitude parameter.

Rest of the paper is organized as follows. In section 2 Fractional Fourier Transform and Time-Frequency (T-F) Analysis are introduced. Various T-F methods are also compared and the use of Chirplet transform is justified in the context of this application. In section 3 the estimation algorithm is explained in details. In addition analogy between discrete computation and continuous results for amplitude estimation is drawn. In section 4 numerical simulations are provided. In section 5 performance of the proposed method in presence of noise is evaluated. Finally in section 6 the paper is concluded with discussions and guideline for future work.

2. Fractional Fourier transform and time-frequency analysis

2.1. Fractional Fourier transform

Fractional Fourier transform (FRFT) is a generalization of Fourier transform and can be viewed as a fractional power of the Fourier operator. The transform also corresponds to a rotation in the time frequency plane.

The concept of Fractional Fourier transform appeared in mathematics as early as 1929. Later it was rediscovered in quantum mechanics, optics and signal processing [6]. In 1980 V. K. Namias [12] established the fact that any linear transform including Fourier transform can be fractionalized, although he was unaware of several previous works.

The definition of continuous Fractional Fourier Transform (CFRFT) of $x(t)$ of order α is defined as [12]

$$F^{\alpha}[x(t)] = X_{\alpha}(u) = \int_{-\infty}^{\infty} x(t)\, k_{\alpha}(t,u)\, dt \tag{1}$$

where

$$k_{\alpha}(t,u) = \begin{cases} C_{\alpha} e^{jat^2 + jau^2 - jbut} & \alpha \neq 0, n\pi \\ \delta(t-u) & \alpha = 0, 4n\pi \\ \delta(t+u) & \alpha = \pi, (4n+2)\pi \end{cases}$$

with $C_\alpha = \sqrt{\frac{1 - j\cot\alpha}{2\pi}}$, $a = \frac{1}{2}\cot\alpha$ and $b = \frac{1}{2}\csc\alpha$, n is an positive or negative integer. Here $\delta(t)$ denotes Dirac-delta function. The Fourier Transform is a special case of FRFT for $\alpha = \frac{\pi}{2}$.

Equation (1) dictates that the transform kernel can be thought as a sequence of following operations [6]:

- Multiplication by a chirp in the reference domain.
- A conventional Fourier transform.
- Frequency scaling by a factor $\csc\alpha$
- Multiplication by a chirp in the transformed domain followed by an amplitude scaling.

Fractional Fourier transform is an orthogonal decomposition of signal into linear chirps having fixed sweep rate $\frac{1}{2}\cot\alpha$, distinguished by a time shift and phase factor such that [6] $k_\alpha(t,u) = k_\alpha(t - u\csc\alpha, 0)$. The chirp decomposition of signals gives FRFT an edge over Fourier Transform for analyzing linear chirp signals, which are extensively used in radar and sonar technology as well as geophysics. The continuous FRFT of a chirp signal $x(t) = \exp(\pm\frac{j}{2}(ct^2 + \mu t))$ is [13],

$$X_\alpha(u) = \begin{cases} \frac{1 + j\tan\alpha}{1 \pm c\tan\alpha} e^{j\frac{u^2(c \mp \tan\alpha) + 2u\mu\csc\alpha \mp u^2\tan\alpha}{2(c\tan\alpha \pm 1)}} & \cot\alpha \neq \pm c \\ \sqrt{1 \mp jc} \times e^{\pm j\frac{cu^2}{2}} \delta(u - \frac{\mu\sin\alpha}{2}) & \cot\alpha = \pm c \end{cases} \quad (2)$$

So, CFRFT of chirp for $\cot\alpha = \pm c$ is a delta function.

Consider the chirp signal $x(t) = \exp(-\frac{j}{2}(1.5t^2 - 6t + 6))$ (3)

The chirp $x(t)$ has sweep rate $c = -1.5$ and initial frequency $\omega_c = 3$. CFRFT of this chirp is shown in Figure 1 for $\alpha = 0$ (time domain), $\alpha = \frac{\pi}{4}$ (fractional domain), $\alpha = \frac{\pi}{2}$ (Fourier domain) and optimal domain ($\cot\alpha = 1.5$). The delta peak for the optimal case is seen at $u = 0.83205$ as expected from equation (2).

The Discrete Fractional Fourier transform (DFRFT) can be defined by discretizing CFRFT with time and fractional domain sampling rate T and U respectively and imposing following constraint on them [13, 14]

$$TU = \frac{2\pi\sin\alpha}{2N+1} \quad (4)$$

Thus DFRFT of $x(nT)$ is defined as

$$X(kU) = e^{j\frac{\cot\alpha}{2}k^2U^2} \sum_{n=-N}^{N} x(nT)\, e^{j\frac{\cot\alpha}{2}n^2T^2} e^{-j\frac{2\pi}{2N+1}kn}, \quad -N \le k \le N \quad (5)$$

where α is the transform order, T and U are the time and fractional domain sampling rate respectively and n and k denotes time and fractional domain sample numbers respectively.

DFRFT defined in equation (5) produces results similar to CFRFT for discrete chirp signals for optimal fractional order. This property is useful for the algorithm described in this paper. The formulation for parameter estimation is provided in later sections. Also an analogy between DFRFT and CFRFT results for chirp signals is also drawn.

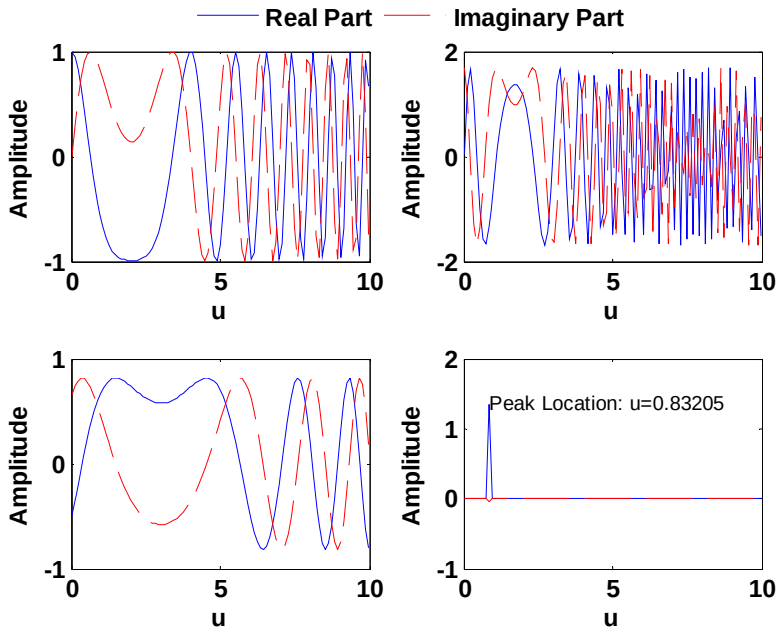

Figure 1. Continuous Fractional Fourier transforms of $x(t)$

2.2. Time-Frequency analysis

Time-Frequency (T-F) analysis refers to the distribution of the energy of a signal simultaneously in time and frequency. The time domain and frequency domain representation of signals are simply subspace of T-F representations.

The T-F analysis was studied thoroughly by D. Gabor in his paper Theory of Communication [15]. The main concept of Gabor analysis was to analyze the signal with windowed sinusoids instead of infinity duration sinusoids. The result was Short-Term Fourier Transform (STFT) defined as

$$STFT[x(t)](\omega,\tau) = \int_{-\infty}^{\infty} x(t)g(t-\tau)e^{-j\omega t}dt \qquad (6)$$

This leads to a tiling of the T-F plane with finite duration (both in time and frequency) "so called" Gabor atoms. Another time frequency representation evolved later which is called wavelet transform [16-19]. Basically it is a time scale representation where the signal is analysed in different scales. The wavelets are produced by a family of translates and dilates of a primitive "Mother Wavelet". The

continuous Wavelet transform has been used for T-F analysis in place of STFT for improved resolution.

Another possible tiling of T-F plane is with atoms which are varying frequency with time. These atoms are short duration chirp signals linearly sweeping their frequency with time. Such T-F atoms give rise to Chirplet transform. An example of such tiling is given in Figure 3. Haykin and Mann introduced the Chirplet transform [20] as a generalization of Wavelet transform in a loose sense where the chirp rate acts as an additional parameter. They proposed a T-F-C volume which constitutes both the Gabor and Wavelet essence with a tiling of chirp like atom. The TFC volume looks like Figure 4.

They further generalized with scaling (dilation) and time-shear and gave rise to a 5-D parameter domain called Chirplet Transform. The Chirplet Transform is defined as [20] the inner product of the signal with a translated (t_c), dilated (Δt), time (d) and frequency (c) sheared short duration chirp signal.

$$S_{t_c,\omega_c,\Delta t,c,d} = \frac{1}{\sqrt{\Delta t}} \int_{-\infty}^{\infty} s(t)\{g^*(\frac{t-tc}{\Delta t}) \otimes e^{-j\frac{d}{2}(\frac{t-tc}{\Delta t})^2}\} e^{-j\frac{c}{2}(\frac{t-tc}{\Delta t})^2} e^{-j\omega_c t}\, dt \qquad (7)$$

Later they proposed several subspace transform from the 5D parameter domain. One of them is Bowtie Chirplet Transform which is used in this paper for chirp parameter estimation.

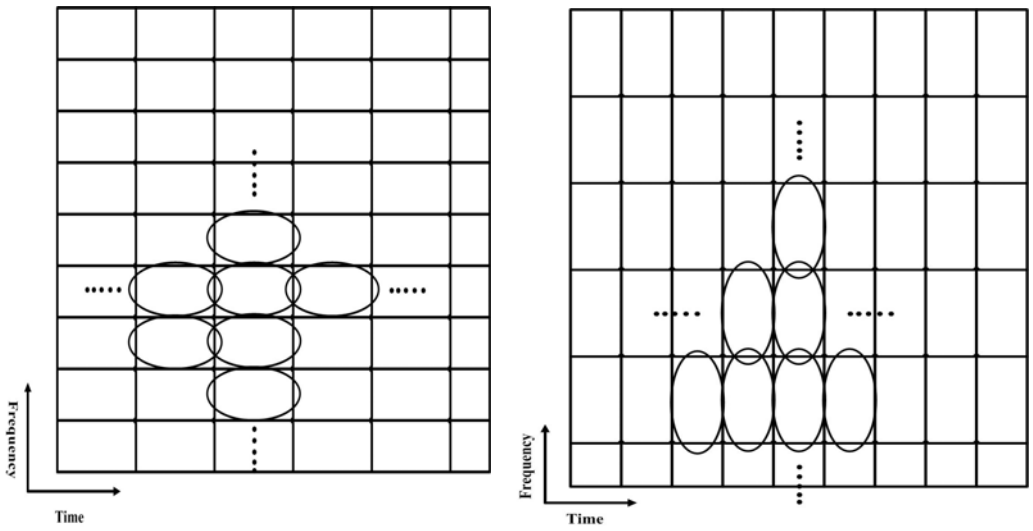

Figure 2. Tiling of T-F plane by Gabor atom; Left: longer duration, shorter bandwidth; Right: shorter duration, longer bandwidth

They further proposed several subspace transform from the 5D parameter domain. One of them is Bowtie Chirplet Transform which is used in this paper for chirp parameter estimation.

2.3. Bowtie Chirplet transform

The Bowtie Chirplet Transform of a signal $x(t)$ is defined by setting $\Delta t = 1$ and d=0.

$$B_X(t_C, \omega_C, c) = \int_{-\infty}^{\infty} x(t)\, e^{-j\frac{1}{2}c(t-t_c)^2} \overline{g(t-t_c)}\, e^{-j\omega_c t}\, dt \tag{8}$$

where t_C, ω_c and c denotes time lag, frequency and chirping (shear) parameters respectively and $g(t)$ is the window function. It is interesting to notice that equation (8) is an extension of Short Time Fourier Transform (STFT) and represents a 1D to 3D mapping of a signal. The name Bowtie came from the shape of the T-F distribution.

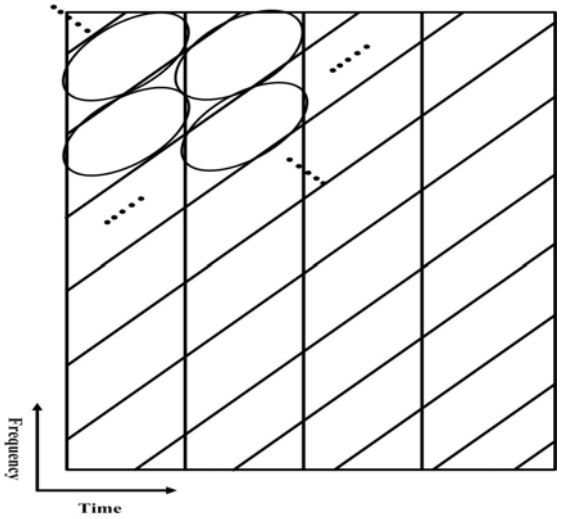

Figure 3. Alternate tiling of T-F plane

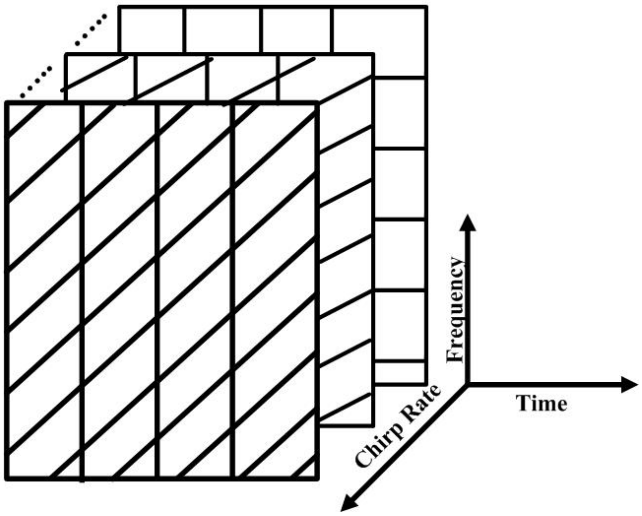

Figure 4. T-F-C volume

2.4 Time-Frequency analysis for chirp rate estimation

Several Time-Frequency techniques, like WVD and Radon Wigner transform have been used for time-frequency analysis of chirp signals.

Wigner-Ville distribution is a quadratic distribution function that has been used in the field radar and sonar signal processing for chirp rate estimation. The Wigner-Ville distribution of a signal $x(t)$ is defines as

$$W[x(t)](t,\omega) = \frac{1}{\sqrt{2\pi}} \int_{-\infty}^{\infty} x(t+\frac{\tau}{2}) x^*(t-\frac{\tau}{2}) e^{-j\omega\tau}\, d\tau \tag{9}$$

where * denotes complex conjugate operation. It represents the time-frequency (t,ω) distribution of a signal. The time-frequency analysis of a linear chirp is a straight line with slope equal to chirp rate. WVD of the $s(t) = a\, e^{j(\frac{1}{2}ct^2 + \gamma t + \phi)}$ is,

$$\begin{aligned} W(t,\omega) &= \frac{1}{\sqrt{2\pi}} \int_{-\infty}^{+\infty} s(t+\frac{\tau}{2}) s^*(t-\frac{\tau}{2}) e^{-j\omega\tau}\, d\tau \\ &= a^2 \delta(\omega - ct - \gamma) \end{aligned} \tag{10}$$

Figure 5(a) shows the WVD for the chirp signal of equation (3) in presence of noise (SNR=-10 dB) and 5(b) schematically shows how sweep rate and initial frequency can be estimated from WVD.

In presence of high noise WVD of chirp is very hard to detect form the noisy background even for a single component as seen in Figure 5(a). Moreover for multi-component signals presence of cross terms makes it even harder. To overcome this problem Radon Transform of WVD (RTW) was proposed to determine chirp rate.

The Radon transform [21] of a 2D function $f(x,y)$ is defined as

$$R_{\rho,\theta}[f(x,y)] = \int_{-\infty}^{\infty}\int_{-\infty}^{\infty} f(x,y)\, \delta(\rho - x\cos\theta - y\sin\theta)\, dx\, dy \tag{11}$$

where $\rho \in [-\infty,\infty]$ and $\theta \in [0,2\pi]$. This transform is simply line integral of the 2D function along different directions. The argument inside the delta function indicates that the integral is taken along straight lines with parameters θ and ρ.

Radon transform of the WVD of chirp is

$$\begin{aligned} \Re(\rho,\theta) &= \int_{-\infty}^{+\infty}\int_{-\infty}^{+\infty} |W(t,\omega)|\, \delta(\rho - t\cos\theta - \omega\sin\theta)\, d\omega\, dt = \frac{1}{|\sin\theta|}\int_{-\infty}^{+\infty} |W(t,-t\cot\theta + \rho\csc\theta)|\, dt \\ &= \frac{1}{|\sin\theta|}\int_{-\infty}^{+\infty} \left| a^2 \delta(\omega - ct - \gamma)\right|_{\omega = -t\cot\theta + \rho\csc\theta} dt = \frac{\csc\theta}{|\cos\theta + c\sin\theta|}\left(\frac{\rho - \gamma\sin\theta}{\cot\theta + c}\right) a^2 \end{aligned} \tag{12}$$

Equation (12) indicates that RTW term will have localized peak at ($\theta = -\cot^{-1} c$, $\rho = \gamma \cos ec\theta$). The integral terms along other lines will be much smaller than this and therefore skipped in this discussion.

Figure 6 shows the RTW for the chirp signal of equation (3). The θ-ρ parameter domain can estimate chirp rate and initial frequency. However, RTW has very high computational complexity and a major draw back is the presence of a large peak at ($\theta = 0^o$, $\rho = 0$) as evident from equation (12) which may cause problem in detection for multi-component signals. Also in some cases the localized peaks tend to deviate from the actual position because of digital

approximations. Chirp peak occurs at ($\theta = -59.13^{o}$, $\rho = 2.893$) which corresponds to estimated $c = -1.673$ and $\omega_c = 2.893$. So a large estimation error is produced for chirp rate in this case.

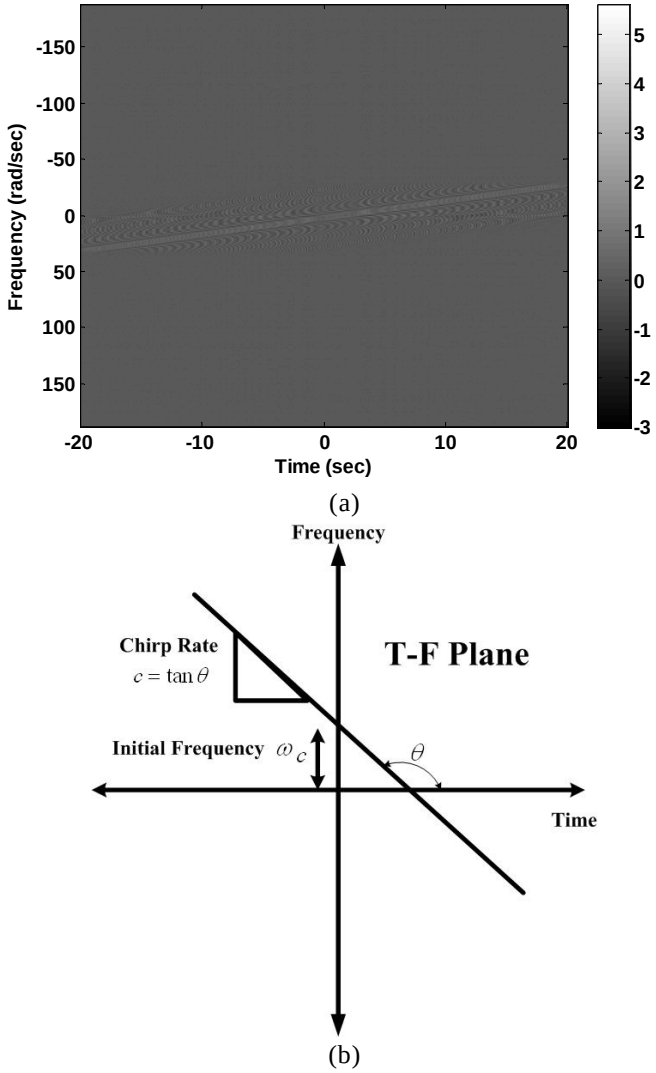

Figure 5. (a)WVD of $x(t)$ (b) Schematic diagram for sweep rate and initial frequency detection

Considering all these factors, in this paper Bowtie chirplet transform is proposed for chirp rate and initial frequency estimation of chirp signal from the chirp rate Vs time lag plane. The peaks can be well localized on the 2D parameter space as shown in Figure 7 for a redefined form of our analyzing signal $x(t) = \exp(-\frac{j}{2}1.5(t-2)^2)$. In this case $t_c = 2$ is the time lag which is related to ω_c as $\omega_c = c\, t_c$. From the peak location $c = -1.5313$ and $\omega_c = 3.0167$ which is more accurate than RTW. Another advantage of Bowtie Chirplet transform is its lesser computational complexity than RTW. Therefore

in this paper Bowtie Chirplet transform is applied for chirp rate and initial frequency estimation and from that result amplitude is estimated from DFRFT

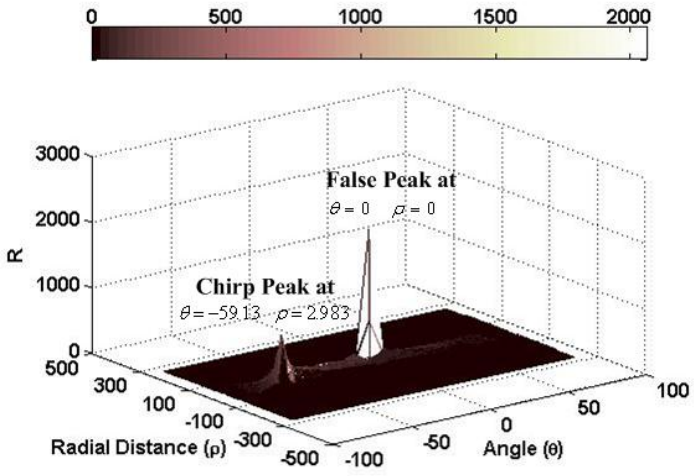

Figure 6. RTW of $x(t)$

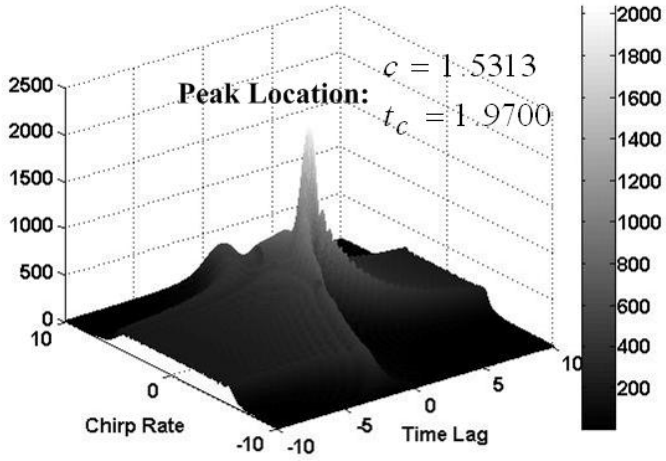

Figure 7. Bowtie Chirplet transform of $x(t)$

3. Proposed estimation method

3.1. Signal model

In this paper the signal is modeled as following.

$$x(t) = \sum_{i=1}^{M} s_i(t) + \mu(t) \tag{13}$$

where $s_i(t)$ is chirp signal defined as

$$s_i(t) = a_i e^{-j\frac{1}{2}c_i(t-\tau_i)^2} \tag{13a}$$

And $S_i^{\alpha}(kU)$ will be denoted as DFRFT of $s_i(t)$.

Here, $\mu(t)$ is zero mean Gaussian noise with known variance σ_μ. a_i is the amplitude parameters and c_i, and τ_i are chirp rate and time lag respectively.

3.2. Phase parameters estimation using Bowtie Chirplet transform

For a signal described as (13) we can write

$$B_X(t_C,\omega_C,c)\Big|_{t_c=\tau_i}^{c=-c_i} = \int_{-\infty}^{\infty} \overline{g(t-t_C)}\, e^{-j\omega_c t}\, dt \tag{14a}$$

That means for such signals the definition is nothing but the Fourier transform of the complex conjugate of arbitrary window function. With simple Fourier properties it can be showed that

$$B_X(t_C,\omega_C,c)\Big|_{t_c=\tau_i}^{c=-c_i} = \overline{G(\omega_C)}\, e^{j\omega_c t} \tag{14b}$$

where $G(\omega_C)$ is the Fourier transform of $g(t)$, and the magnitude response will be obviously

$$\left|B_X(t_C,\omega_C,c)\Big|_{t_c=\tau_i}^{c=-c_i}\right| = |G(\omega_C)| \tag{14c}$$

Now irrespective of the type of window function its magnitude spectrum will be maximum at $\omega_C = 0$. Thus for this special type of signal we can modify (or rather simplify) the definition as

$$B_X(t_C,0,c) \equiv B_X(t_C,c) = \int_{-\infty}^{\infty} x(t)\, e^{-j\frac{1}{2}c(t-\tau_i)^2} \overline{g(t-t_C)}\, dt \tag{14d}$$

This can be further re-written as

$$B_X(t_C,c) = \int_{-\infty}^{\infty} x(t)\, \overline{e^{j\frac{1}{2}c(t-\tau_i)^2} g(t-t_C)}\, dt = \int_{-\infty}^{\infty} x(t)\, \overline{\tilde{g}(t-t_C)}\, dt \tag{14e}$$

Equation (14d) is in effect the cross-correlation between $x(t)$ and $\tilde{g}(t) = g(t)\, e^{-j\frac{c}{2}t^2}$. The cross-correlation can be efficiently performed taking c as parameter using Fast Fourier Transform (FFT) algorithm and phase parameters can be estimated from the fact that peak will be observed on the (t_C, c) plane at (τ_i, c_i).

3.3. Amplitude parameter estimation using Discrete Fractional Fourier Transform (DFRFT)

Two basic theorems are proposed in this section for estimating amplitude parameter using DFRFT. Also an analogy with CFRFT is provided.

3.3.1. Theorem 1

For a discrete signal, $x(nT) = A\exp(\frac{j}{2}c(nT-f)^2)$, the magnitude DFRFT spectrum will be,

$$|X_\alpha(kU)| = \begin{cases} (2N+1)A & k = k_0 \quad \& \quad c = -\cot\alpha \\ 0 & k \neq k_0 \quad \& \quad c = -\cot\alpha \\ A\left|\sum_{n=-N}^{N} \exp\{-j\theta_n\}\right| \leq (2N+1)A & c \neq -\cot\alpha \end{cases} \tag{15}$$

where $\theta_n = \frac{2\pi}{2N+1}(k-k_0) - \frac{(c+\cot\alpha)n^2T^2}{2}$

T is the sampling rate

$k_0 = \frac{2N+1}{2\pi} T f c$ is an integer

Theorem 1 states that for a chirp signal $x(nT)$, if the term $\frac{2N+1}{2\pi} T f c = k_0$ is integer then, a delta peak will be visible at $k = k_0$ for optimal angle $c = -\cot\alpha$. The inequality indicates that the delta peak will be largest peak in Fractional Fourier domain.

Proof: Following the definition of DFRFT,

$$X_\alpha(kU) = A\exp(\frac{j}{2}k^2U^2\cot\alpha) \sum_{n=-N}^{N} x(nT)\exp(\frac{j}{2}n^2T^2\cot\alpha)\exp(-j\frac{2\pi}{2N+1}nk) \tag{16a}$$

Upon replacing $x(nT)$ and simplifying,

$$X_\alpha(kU) = A\exp(\frac{j}{2}cf^2)\exp(\frac{j}{2}k^2U^2\cot\alpha) \sum_{n=-N}^{N} \exp(\frac{j}{2}(c+\cot\alpha)n^2T^2)\exp(-j\frac{2\pi n}{2N+1}(k-\frac{2N+1}{2\pi}Tfc)) \tag{16b}$$

Now let $k_0 = \frac{2N+1}{2\pi}Tfc$ an integer number. Hence,

Case 1: $k = k_0 \quad \& \quad c = -\cot\alpha$

$$X_\alpha(kU) = A\exp(\frac{j}{2}cf^2)\exp(-c\frac{j}{2}k_0{}^2U^2) \sum_{n=-N}^{N}(1) = A\exp(\frac{j}{2}cf^2)\exp(-c\frac{j}{2}k_0{}^2U^2)(2N+1)$$

$$|X_\alpha(kU)| = (2N+1)A$$

Case 2: $k \neq k_0 \quad \& \quad c = -\cot\alpha$

Starting from equation (16b)

$$X_\alpha(kU) = A\exp(\frac{j}{2}cf^2)\exp(\frac{j}{2}k^2U^2\cot\alpha) \sum_{n=-N}^{N} \exp(-j\frac{2\pi n}{2N+1}(k-k_0)) \tag{16c}$$

Let $a = \exp(-j\frac{2\pi n}{2N+1}(k-k_0))$

Therefore,

$$X_\alpha(kU) = A\exp(\frac{j}{2}cf^2)\exp(-c\frac{j}{2}k^2U^2) \sum_{n=-N}^{N} a^n = A\exp(\frac{j}{2}cf^2)\exp(-c\frac{j}{2}k^2U^2)\frac{1-a^{2N+1}}{1-a} \tag{16d}$$

Since $k-k_0$ is an integer, $a^p=1$ for all integers p
Thus $X_\alpha(kU)=0$

Case 3: $c\neq-\cot\alpha$

Again starting from equation (16b)

$$X_\alpha(kU)=A\exp(\frac{j}{2}cf^2)\exp(\frac{j}{2}k^2U^2\cot\alpha)\sum_{n=-N}^{N}\exp(\frac{j}{2}(c+\cot\alpha)n^2T^2)\exp(-j\frac{2\pi n}{2N+1}(k-k_0))$$

$$\therefore\left|X_\alpha(kU)\right|=A\left|\sum_{n=-N}^{N}\exp\{-j(\frac{2\pi n}{2N+1}(k-k_0)-\frac{c+\cot\alpha}{2}n^2T^2)\}\right|=A\left|\sum_{n=-N}^{N}\exp\{-j\theta_n\}\right|=A\times\arg\left[\sum_{n=-N}^{N}\exp\{-j\theta_n\}\right]$$

$$\leq A\times\sum_{n=-N}^{N}\arg\left[\exp\{-j\theta_n\}\right]$$

$$\leq A(2N+1)$$

(16e)

where $$\theta_n=\frac{2\pi}{2N+1}(k-k_0)-\frac{(c+\cot\alpha)n^2T^2}{2}$$

3.3.2. Theorem 2

For a discrete signal, $x(nT)=A\exp(\frac{j}{2}c(nT-f)^2)$, the magnitude DFRFT spectrum will be,

$$\left|X_\alpha(kU)\right|=\begin{cases}(2N+1)A\dfrac{\sin c(\in)}{\sin c(\dfrac{\in}{2N+1})} & k=\hat{k}_0=k_0\pm\in \quad\&\quad c=-\cot\alpha\\ A(2N+1)\dfrac{\sin c(k-\hat{k}_0\mp\in)}{\sin c(\dfrac{k-\hat{k}_0\mp\in}{2N+1})} & k\neq\hat{k}_0=k_0\pm\in \quad\&\quad c=-\cot\alpha\end{cases}$$

(17)

where $$\theta_n=\frac{2\pi}{2N+1}(k-k_0)-\frac{(c+\cot\alpha)n^2T^2}{2}$$

T is the sampling rate

$k_0=\dfrac{2N+1}{2\pi}Tfc$ is non-integer

$\hat{k}_0$ is the nearest possible integer of k_0

$\in$ is a small real number

Theorem 2 states that for a chirp signal $x(nT)$, if the term $\dfrac{2N+1}{2\pi}T\,f\,c=k_0$ is non-integer then, a peak, corresponding to sinc function main lobe, will be visible at nearest integer $k=\hat{k}_0$ for optimal angle $c=-\cot\alpha$. However for other $k\neq\hat{k}_0$ the side lobes will be visible.

This Theorem is indeed important when $\frac{2N+1}{2\pi}Tfc$ is not an integer. In that case still a Peak is produced at the nearest integer index of DFRFT ($\hat{k}_0$) and amplitude can be located according to equation (17).

Proof: Starting from equation (16b)

$$X_\alpha(kU) = A\exp(\frac{j}{2}cf^2)\exp(\frac{j}{2}k^2U^2\cot\alpha)\sum_{n=-N}^{N}\exp(\frac{j}{2}(c+\cot\alpha)n^2T^2)\exp(-j\frac{2\pi n}{2N+1}(k-k_0))$$

And replacing $k_0 = \hat{k}_0 \pm \in$

$$X_\alpha(kU) = A\exp(\frac{j}{2}cf^2)\exp(\frac{j}{2}k^2U^2\cot\alpha)\sum_{n=-N}^{N}\exp(\frac{j}{2}(c+\cot\alpha)n^2T^2)\exp(-j\frac{2\pi n}{2N+1}(k-\hat{k}_0\mp\in)) \tag{18a}$$

Case 1: $k=\hat{k}_0$ & $c=-\cot\alpha$

$$X_\alpha(kU) = A\exp(\frac{j}{2}cf^2)\exp(\frac{j}{2}\hat{k}_0^2U^2\cot\alpha)\sum_{n=-N}^{N}\exp(\mp j\frac{2\pi n}{2N+1}\in) \tag{18b}$$

Let $b=\exp(\mp j\frac{2\pi n}{2N+1}\in)$

Therefore,

$$\begin{aligned}
X_\alpha(kU) &= A\exp(\frac{j}{2}cf^2)\exp(\frac{j}{2}\hat{k}_0^2U^2\cot\alpha)\sum_{n=-N}^{N}b^n \\
&= A\exp(\frac{j}{2}cf^2)\exp(\frac{j}{2}\hat{k}_0^2U^2\cot\alpha)\frac{1-b^{2N+1}}{1-b} \\
&= A\exp(\frac{j}{2}cf^2)\exp(\frac{j}{2}\hat{k}_0^2U^2\cot\alpha)\frac{1-\exp(\pm j2\pi\in)}{1-\exp(\pm\frac{j2\pi\in}{2N+1})} \\
&= \pm A\exp(\frac{j}{2}cf^2)\exp(\frac{j}{2}\hat{k}_0^2U^2\cot\alpha)\exp(\mp j\frac{2\pi N}{2N+1}\in)\frac{\sin(\pi\in)}{\sin(\frac{\pi\in}{2N+1})}
\end{aligned} \tag{18c}$$

So, $|X_\alpha(kU)| = A\frac{\sin(\pi\in)}{\sin(\frac{\pi\in}{2N+1})} = (2N+1)A\frac{\sin c(\in)}{\sin c(\frac{\in}{2N+1})}$

Case 2: $k\neq\hat{k}_0$ & $c=-\cot\alpha$

Similar to case 2 Theorem 1 it can be shown,

$$X_\alpha(kU) = A\exp(\frac{j}{2}cf^2)\exp(\frac{j}{2}k^2U^2\cot\alpha)\frac{\sin\pi(k-\hat{k}_0\mp\in)}{\sin\frac{\pi}{2N+1}(k-\hat{k}_0\mp\in)}$$

$$\therefore |X_\alpha(kU)| = A(2N+1)\frac{\sin c(k-\hat{k}_0\mp\in)}{\sin c(\frac{k-\hat{k}_0\mp\in}{2N+1})}$$

For $\in\to 0$ Theorem 2 converges to Theorem 1

Therefore theorem 1 & 2 indicates that if the chirp rate and time lag (as well as initial frequency) Parameters are already known DFRFT can estimate amplitude parameter of $s_i(t)$ at optimal angle using following magnitude spectra relation

$$a_i \cong \frac{\left|S_i{}^\alpha(kU)\right|_{k=k_0}}{(2N+1)} \tag{19}$$

3.3.3. Analogy between CFRFT and DFRFT

For a windowed continuous chirp signal $\tilde{x}(t) = x(t)w(t)$, where $w(t) = rect(\frac{t}{2L})$

$$X_\alpha(u) = AC_\alpha\exp(\frac{j}{2}\cot\alpha\,u^2)\int_{-L}^{L}\exp(\frac{j}{2}c(t-f)^2)\exp(\frac{j}{2}\cot\alpha\,t^2)\exp(-j\csc\alpha\,ut)\,dt$$

$$= AC_\alpha\exp(\frac{j}{2}\cot\alpha\,u^2)\exp(\frac{j}{2}cf^2)\int_{-L}^{L}\exp(\frac{j}{2}(\cot\alpha+c)t^2)\exp(-j(\csc\alpha\,u+cf)t)\,dt \tag{20a}$$

For $c = -\cot\alpha$

$$X_\alpha(u) = AC_\alpha\exp(-\frac{j}{2}c(u^2-f^2))\int_{-L}^{L}\exp(-j(\csc\alpha\,u+cf)t)\,dt$$

$$= AC_\alpha\exp(-\frac{j}{2}c(u^2-f^2))\frac{\exp(-j(\csc\alpha\,u+cf)L)-\exp(j(\csc\alpha\,u+cf)L)}{-j(\csc\alpha\,u+cf)}$$

$$= AC_\alpha\exp(-\frac{j}{2}c(u^2-f^2))\frac{-2j\sin((\csc\alpha\,u+cf)L)}{-j(\csc\alpha\,u+cf)L}L$$

$$= ALC_\alpha\exp(-\frac{j}{2}c(u^2-f^2))\sin c((\csc\alpha+cf)L)$$

$$\therefore |X_\alpha(u)| = AL\times\sin c((\csc\alpha+cf)L) \tag{20b}$$

For $c\neq-\cot\alpha$

$$X_\alpha(u) = AC_\alpha \exp(\frac{j}{2}\cot\alpha u^2)\exp(\frac{j}{2}cf^2)\int_{-L}^{L}\exp\{\frac{j}{2}(\cot\alpha+c)(t^2-\frac{\csc\alpha u+cf}{\cot\alpha+c}t)\}dt$$
$$= AC_\alpha \exp(\frac{j}{2}\cot\alpha u^2)\exp(\frac{j}{2}cf^2)\exp\{-\frac{j}{2}\frac{(\csc\alpha u+cf)^2}{\cot\alpha+c}\}\int_{-L}^{L}\exp\{\frac{j}{2}(\cot\alpha+c)(t-\frac{\csc\alpha u+cf}{\cot\alpha+c})^2\}dt \quad (20c)$$

With some change of variable and further simplifying,

$$X_\alpha(u) = AC_\alpha \exp(\frac{j}{2}\cot\alpha u^2)\exp(\frac{j}{2}cf^2)\int_{-L}^{L}\exp\{\frac{j}{2}(\cot\alpha+c)(t^2-\frac{\csc\alpha u+cf}{\cot\alpha+c}t)\}dt$$
$$= AC_\alpha \exp(\frac{j}{2}\cot\alpha u^2)\exp(\frac{j}{2}cf^2)\exp\{-\frac{j}{2}\frac{(\csc\alpha u+cf)^2}{\cot\alpha+c}\}\int_{-L}^{L}\exp\{\frac{j}{2}(\cot\alpha+c)(t-\frac{\csc\alpha u+cf}{\cot\alpha+c})^2\}dt$$
$$= AC_\alpha \frac{2j}{\cot\alpha+c}\exp\{\frac{j}{2}(\cot\alpha u^2+cf^2)\}\exp\{-\frac{j}{2}\frac{(\csc\alpha u+cf)^2}{\cot\alpha+c}\}\left[\int_0^{\sigma}\exp(-jy^2)dy-\int_0^{\delta}\exp(-jy^2)dy\right] \quad (20d)$$

where

$$\delta = -(\frac{\cot\alpha+c}{1-j})(L+\frac{\csc\alpha u+cf}{\cot\alpha+c}) \qquad \sigma = (\frac{\cot\alpha+c}{1-j})(L-\frac{\csc\alpha u+cf}{\cot\alpha+c})$$

Now using Fresnel Integral,

$$F(\beta) = \int_0^{\beta}\exp(-jy^2)dy = \sum_{n=0}^{\infty}(-1)^n\frac{\beta^{4n+1}}{(4n+1).2n!} - j\sum_{n=0}^{\infty}(-1)^n\frac{\beta^{4n+3}}{(4n+3).(2n+1)!} \quad (20e)$$

$$X_\alpha(u) = AC_\alpha \frac{2j}{\cot\alpha+c}\exp\{\frac{j}{2}(\cot\alpha u^2+cf^2)\}\exp\{-\frac{j}{2}\frac{(\csc\alpha u+cf)^2}{\cot\alpha+c}\}[F(\alpha)-F(\delta)] \quad (20f)$$

Thus CFRT for windowed chirp signals with optimal angle produce sinc function main lobe depending on the initial frequency. This property is similar to the DFRFT case.

4. Simulation results

The proposed estimation method is investigated with numerical simulation. The test signal is composed of four linear chirp signals. The parameters are:

$$(1)\, c_1 = 3, \tau_1 = 4.7, a_1 = 2.54 \qquad (2)\, c_2 = -3.3, \tau_2 = -2.64, a_2 = 3.11$$
$$(3)\, c_3 = 1.4, \tau_3 = 0, a_3 = 2.41 \qquad (4)\, c_4 = 5.7, \tau_4 = -4.70, a_2 = 4.62$$

Rectangular window $w(n) = rect(\frac{nT}{2001})$ is chosen with T=0.01.Figure 8 shows the 2D Chirplet Transform result (c vs. t_c) for estimation of c and τ at SNR=-10 dB. The peaks are found at (3,4.71), (-3.2, -2.65), (1.38,0) and (5.7,-4.69).

DFRFT results for $\alpha = -\cot^{-1} 3$, $\alpha = \cot^{-1} 3.2$, $\alpha = -\cot^{-1} 1.4$ and $\alpha = -\cot^{-1} 5.7$ are shown in Figure 9. The values of a_i estimated from equation (19) are 2.7069, 2.993 respectively. Figure 10 presents the actual noisy and estimated signal for this noise level.

5. Performance analysis and discussion

To evaluate the performance of the system under noise, Monte-Carlo simulations are performed. Components 1 & 2 are used from previous section.

The estimation values are computed 100 times for each of a_i for each case of SNR=-10 dB,-8 dB, -6dB,-4dB,-2 dB, 0dB, 2 dB, 4dB, 6 dB, 8 dB and 10 dB. The accuracy of estimation is measured as Mean Squared Error (MSE),

$$MSE = 10 \log_{10} [\frac{1}{M} \sum_{i=1}^{M} (\hat{p}_i - p)^2] \quad dB \tag{21}$$

where $\hat{p}_i$ denote the estimated value of parameter p at the i_{th} computation and M is the number of Monte-Carlo computation. Figure 11 shows the MSE of estimated amplitude parameters for various SNR. The estimated values for chirp rate and initial frequency parameters are constant over this range of SNR and hence are not shown.

6. Conclusions

A sequential estimation method combining Bowtie Chirplet Transform and Discrete Fractional Fourier transform (DFRFT) is proposed. The former is capable of estimating chirp rate and initial frequency in very low SNR. The DFRFT enables to compute the amplitude parameter. The proposed method is well suited for applications involving multiple-parameter estimation of chirp signals. The algorithm is tested for several noise levels with Monte-Carlo simulation. However, Cramer-Rao lower bound (CRB) for the estimation is required to be derived and compared with Monte-Carlo simulation result. Also similar estimation method for linear amplitude modulated chirp signals can be investigated. Effectiveness of this proposed method for real world application (speech modeling and synthesis, for example) is yet to be performed and therefore attributed to future work.

7. References

[1] Y. Huang, and R.D. Dony, “Speech modelling by non-stationary partials with time varying amplitude and frequency”, Electrical and Computer Engineering, 2004. Canadian Conference on, Vol.3, 2-5 May 2004, pp. 1273-1276.
[2] S. Barbarossa, and A. Farina, “Detection and imaging of moving objects with synthetic aperture radar 2: Joint time-frequency analysis by Wigner-Ville distribution”, Radar and Signal Processing, IEE Proceedings, Vol.139, No.1, Feb 1992, pp.89-97.
[3] J.C. Wood, and D.T. Barry, “Radon transformation of time-frequency distributions for analysis of multicomponent signals”, Signal Processing, IEEE Transactions on, Vol.42, No.11, Nov 1994, pp.3166-3177.
[4] M. Wang; A.K. Chan, and C.K. Chui, “Linear frequency-modulated signal detection using Radon-ambiguity transform”, Signal Processing, IEEE Transactions on, Vol.46, No.3, Mar 1998, pp.571-586.
[5] Z. Xinghao, T. Ran, and Z. Siyong, “A novel sequential estimation algorithm for chirp signal parameters”, Neural Networks and Signal Processing, 2003. Proceedings of the 2003 International Conference on, Vol.1, 14-17, Dec. 2003, pp. 628-631.
[6] L.B. Almeida,”The fractional Fourier transform and time-frequency representations”, Signal Processing, IEEE Transactions on, Vol.42, No.11, Nov 1994, pp.3084-3091.
[7] H.M. Ozaktas, O. Arikan, M.A. Kutay, and G. Bozdagt, “Digital computation of the fractional Fourier transform”, Signal Processing, IEEE Transactions on, Vol.44, No.9, Sep 1996, pp.2141-2150.

[8] M.M. Wang, A.K. Chan, and C.K. Chui, "Linear frequency modulated signal detection using wavelet packet, ambiguity function and Radon transform", Antennas and Propagation Society International Symposium, 1995. AP-S. Digest, Vol.1, 18-23 Jun 1995, pp.308-311.
[9] Z. Huafeng, Z. Jianping, and H.J. Guo, "Instantaneous parameter estimation based on continuous wavelet transform and some improvements", Acoustics, Speech and Signal Processing, 1998. Proceedings of the 1998 IEEE International Conference on, Vol.4, 12-15 May 1998, pp.2169-2172.
[10] S. Peleg, and B. Friedlander, "The discrete polynomial-phase transform", Signal Processing, IEEE Transactions on, Vol.43, No.8, Aug 1995, pp.1901-1914.
[11] Xiang-Gen Xia, "Discrete chirp-Fourier transform and its application to chirp rate estimation", Signal Processing, IEEE Transactions on, Vol.48, No.11, Nov 2000, pp.3122-3133.
[12] V. Namias, "The fractional order Fourier transform and its application to quantum mechanics", J. Inst. Math. Appl., Vol. 25, 1980, pp. 241–265.
[13] N. A. Siddique, A. Mostayed and S. Z. K. Sajib, Discrete Fractional Fourier Transform with Applications in Signal Processing, BSc. Thesis, Dept. of Electrical and Electronic Engineering, Bangladesh University of Engineering and Technology, Dhaka, June 2007.
[14] S.C. Pei, and J.J. Ding, "Closed-form discrete fractional and affine Fourier transforms", Signal Processing, IEEE Transactions on, Vol.48, No.5, May 2000, pp.1338-1353.
[15] D. Gabor, "Theory of communication", J. IEE, Vol. 93, 1946, pp. 429-457.
[16] C. Heil, and D. F. Walnut, "Continuous and discrete wavelet transforms", SIAM Rev., Vol. 31, No. 4, Dec. 1989, pp. 628-666.
[17] S.G. Mallat, "A theory for multiresolution signal decomposition: the wavelet representation", Pattern Analysis and Machine Intelligence, IEEE Transactions on, Vol.11, No.7, Jul 1989, pp. 674-693.
[18] I. Daubechies, "The wavelet transform, time-frequency localization and signal analysis", Information Theory, IEEE Transactions on , Vol.36, No.5, Sep 1990, pp. 961-1005.
[19] G. Strang, "Wavelets and dilation equations: a brief introduction", SIAM Rev., Vol. 31, No. 4, Dec. 1989, pp. 614-627.
[20] S. Mann, and S. Haykin, "The chirplet transform: physical considerations", Signal Processing, IEEE Transactions on, Vol. 43, No. 11, Nov 1995, pp. 2745-2761.
[21] J.C. Wood, and D.T. Barry, "Tomographic time-frequency analysis and its application toward time-varying filtering and adaptive kernel design for multicomponent linear-FM signals", Signal Processing, IEEE Transactions on, Vol.42, No.8, Aug 1994, pp.2094-2104.

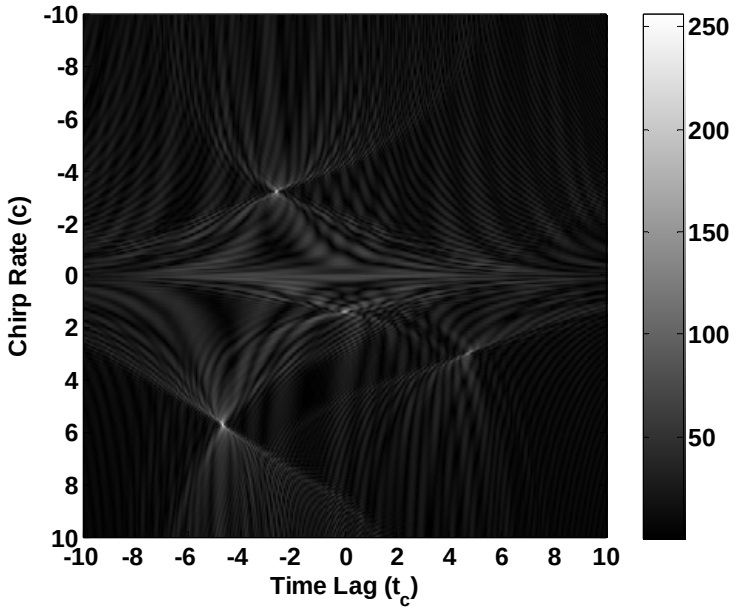

Figure 8. Bowtie Chirplet transform of the test signal. Values are mapped onto the range 0 to 255

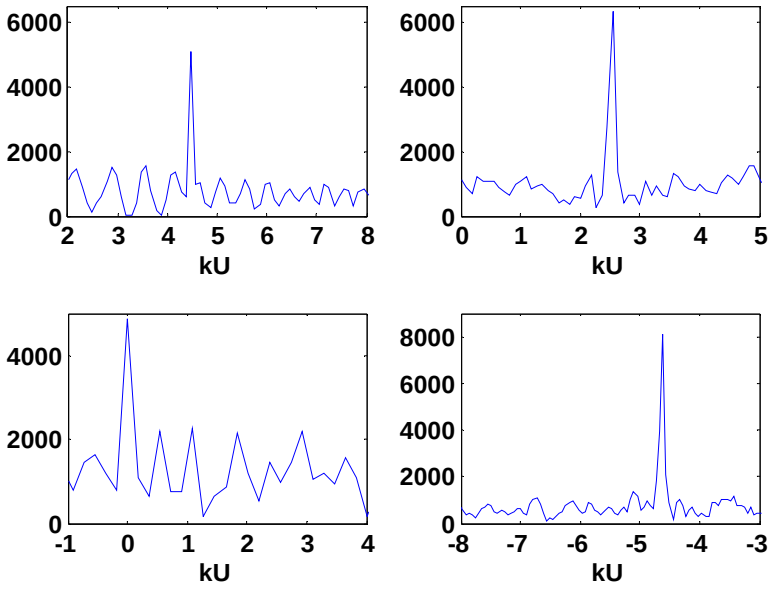

Figure 9. DFRFT Magnitude of test signal for $\alpha = -\cot^{-1} 3$, $\alpha = \cot^{-1} 3.2$, $\alpha = -\cot^{-1} 1.4$ and $\alpha = -\cot^{-1} 5.7$

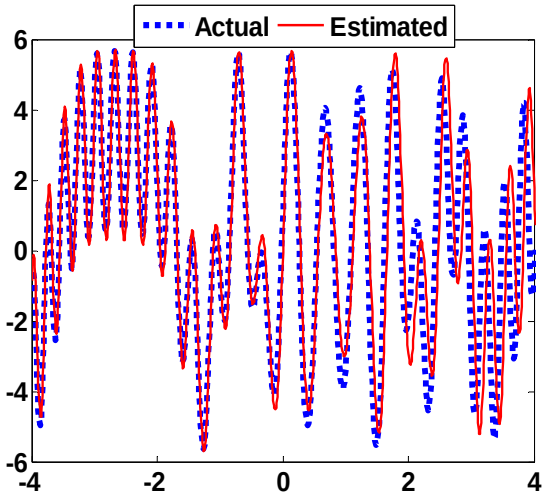

Figure 10. Real parts of the simulated chirp signal and reconstructed chirp signal on the same plot

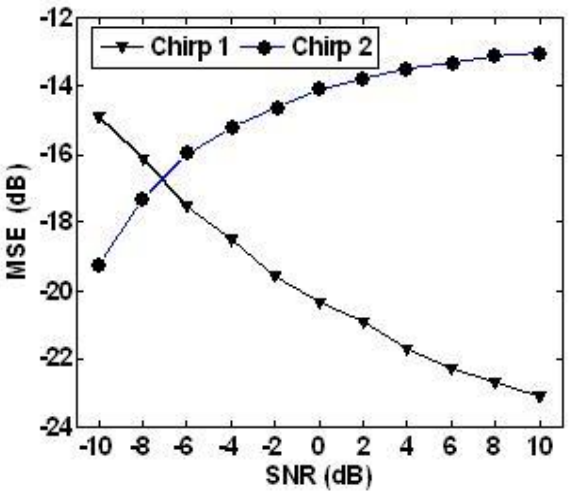

Figure 11. MSE vs. SNR plot for parameter estimation of the test signal

Authors

Ahmed Mostayed received his B.Sc. degree in Electrical and Electronic Engineering from Bangladesh University of Engineering and Technology (BUET) and currently pursuing M.Sc. in Electrical Engineering at Kongju National University, South Korea. His current research interests are biometric authentication and identification, pattern recognition and signal processing.

Saurav Zaman Khan Sajib received his B.Sc. degree in Electrical and Electronic Engineering from Bangladesh University of Engineering and Technology (BUET). Currently he is working as Engineer at Alcatel-Lucent France Bangladesh Branch at Wireless Transmission Department (WTD). His current research interest includes image processing, digital signal processing and pattern recognition.

Sikyung Kim received his B. S. and M. S. degree in Electrical Engineering from Korea University in 1986 and 1988 respectively. He completed his Ph.D. Degree from Texas A&M in June 1994. He joined Kongju National University, South Korea in 1994 and currently a Professor with the Department of Electrical Engineering. His research interests are embedded systems, biomechanics, sensor network, computer aided designs and power electronics.